RSC Advances

PAPER

View Article Online
View Journal | View Issue

Cite this: *RSC Adv.*, 2025, **15**, 34128

Analytical green star area (AGSA) as a new assessment tool for the electrochemical determination of cyclobenzaprine hydrochloride in wastewater samples using recycled graphite-modified nitrogen-doped CQDs

Hamdy Khamees Thabet,[ab] Ashraf M. Ashmawy,[c] Mohamed A. Ali,[d] Ebrahim A. El-Desouky[e] and Ahmed M. Abdel-Raoof[*e]

Received 8th July 2025
Accepted 31st August 2025

DOI: 10.1039/d5ra04880j

rsc.li/rsc-advances

Active pharmaceutical compound consumption and their discharge into municipal wastewater *via* excretion are a growing danger for water quality and have considerable short-term, medium-term, and long-term impacts on environmental and human health. The objectives of this work were the detection and determination of cyclobenzaprine hydrochloride (CBZ), the most used muscle relaxant present in wastewater, with high accuracy and precision to avoid the serious environmental threat caused by the medication's overuse. The proposed electrode showed higher sensitivity with a Nernstian slope value of 57.97 ± 0.23 mV per decade in the linearity range of 1.0×10^{-7} to 1.0×10^{-2} M and an LOD of 5.62×10^{-8}. This study is also the first to corroborate the use of a graphite electrode prepared from battery rod waste for the determination of CBZ, along with modification with nitrogen-doped carbon quantum dots derived from pea pods, and L-serine amino acid (PP-NCQDs) as the indicator electrode. Using molecular docking, the α-CD ionophore was found to be the most favorable orientation of CBZ towards the highly selective ionophore in the membrane sensor. The open source and accessible nature of the Analytical Green Star Area (AGSA) facilitates cross-disciplinary comparisons.

1. Introduction

Water has been utilized in various capacities within the domestic, industrial, and agricultural contexts. Such applications have led to the introduction of numerous undesirable compounds and pollutants into wastewater systems.[1] In recent years, the detection of pharmaceutical residues within aquatic ecosystems has been documented globally.[2] Nevertheless, current studies suggest their determination is critical as these pollutants represent significant risks, albeit at considerable concentrations, to the environment, wildlife, and human health.[3] The total amount of pharmaceuticals that are discharged into the sewage system and the lack of suitable wastewater treatment techniques to address this problem result in high levels of pharmaceuticals in drinking water. Owing to their limited degradability, approximately 80% of these compounds are excreted unmodified and subsequently disposed of *via* toilets and sewer systems directed towards wastewater treatment facilities, where no effective removal occurs, thereby fostering the proliferation of bacterial resistance.[4] This situation results in increased levels of pharmaceuticals in drinking water, which are assimilated by individuals, thereby exacerbating the challenges associated with the treatment of prevalent health conditions and their determination.[4]

High-performance carbon quantum dots (CQDs), which have several uses, such as sensing, are increasingly in demand. Nevertheless, there are still issues with the synthesis of CQDs, such as the use of toxic materials, protracted multistep procedures, and high costs.[5,6] As renewable resources that are good for the environment, biomass and biomass waste (such as agricultural products, agricultural residue, and municipal solid waste) are plentiful and have a high carbon content (45–55%).[7,8]

In this paper, we report the use of a microwave-assisted process to successfully synthesize N-doped carbon quantum dots (NCQDs) from pea pods, which are an abundant, readily available, cost-effective biomass carbon source, and L-serine amino acid is used as a nitrogen dopant.

Molecular docking (MO), a methodology for predicting new indications of current medications, is a useful technique for

[a]*Center for Scientific Research and Entrepreneurship, Northern Border University, Arar, 73213 Saudi Arabia*
[b]*Department of Chemistry, College of Sciences and Arts, Northern Border University, Rafha, 91911 Saudi Arabia*
[c]*Chemistry Department, Faculty of Science (boys), Al-Azhar University, 11884, Egypt*
[d]*School of Biotechnology, Badr University in Cairo (BUC), Badr City, Cairo 11829, Egypt*
[e]*Pharmaceutical Analytical Chemistry Department, Faculty of Pharmacy, Al-Azhar University, 11751, Nasr City, Cairo, Egypt. E-mail: Ahmedmeetyazeed79@Azhar.edu.eg*

developing treatments for new diseases, especially rare ones, while cutting down on the time and expense of drug development. Potential target identification is an essential stage in the process of finding novel indications. Molecular docking is a popular technique for finding possible targets for a particular drug or finding potential drugs for a specific target, and it doesn't require any prior knowledge other than structure inputs from the drug and the target.[9] Recently, MD has been used for aiding in the determination of some pharmaceutical compounds by studying the interaction between the drug target and the ionophore as binding site receptors; the greater the binding interaction between them, the more appropriate they are for the methodology.[10–12]

Cyclobenzaprine HCl (CBZ) acts centrally as a skeletal muscle relaxant related to tricyclic antidepressants.[13] The determination of CBZ is described in previous studies by the U.S. Pharmacopeia,[14] and others *via* spectrophotometry[15,16] and liquid and gas chromatography.[17–21] However, these reported methods involve expensive equipment, significant sample preparation, long analysis times, and organic solvents. Electrochemical techniques, particularly voltammetry[22–25] and potentiometry,[26–28] have been suggested as available alternatives. These techniques are known for their high sensitivity, speed, simplicity, selectivity, cost-effectiveness, and eco-friendliness.

In this study, we present the Analytical Green Star Area (AGSA), which is open source and accessible at **https://www.bit.ly/AGSA2025** as an extension of the Green Star Area index, aimed at assessing the green analytical determination of CBZ, while placing significant emphasis on analytical methodologies. This innovative metric facilitates the assessment of the twelve principles of green analytical chemistry (GAC), providing a visual representation of the overall environmental ramifications. The increased green area associated with an analytical methodology within AGSA correlates with a heightened level of greenness. Consequently, AGSA serves as a valuable instrument for analytical chemists, permitting the rapid and straightforward comparisons of various chemical processes and directing enhancements towards more sustainable analytical practices.[29]

The major reason for the presence of cyclobenzaprine (CBZ) and other pharmaceuticals in surface water and groundwater is their entry into the waters *via* human excrement and the inadequate disposal of expired or unused drugs. The determination of different pharmaceutical substances and pharmaceutical content in both treated wastewater and sewage sludge is difficult owing to the complex composition of this matrix. As such, a highly selective and sensitive electrode made of waste graphite modified with PP-NCQDs for the determination of CBZ is applicable due to its being non-toxic, inexpensive, and having favorable electrochemical characteristics, including a large surface area and excellent electrical conductivity.

2. Experimental

2.1. Chemicals and reagents, instrumentation, and software

See the SI for details.

2.2. Procedures

2.2.1. Microwave-assisted synthesis of PP-NCQDs. The seeds of the fresh green pea pods were extracted from their respective casings, after which the vacated pods were gathered and washed with distilled water to eliminate any residual matter. The desiccated pods were subsequently sectioned into small fragments and homogenized using a domestic fruit mixer to yield a uniform matrix. The resultant mixture (10 g) was mixed with 50 mg L-serine and subjected to treatment in a domestic microwave at a power setting of 900 W for a duration of 9 minutes, after which it was allowed to cool to ambient temperature. A volume of fifteen milliliters of distilled water was incorporated into 100 mg of the resultant black residue within a 100 mL beaker, followed by sonication for a period of 30 minutes, and subsequently filtered. The filtrate underwent centrifugation for 10 minutes at a rotational speed of 4000 rpm. The brownish-yellow suspension was further filtered through a 0.45 μm syringe filter to isolate the nitrogen-doped carbon quantum dot solution. The resulting dark brownish-yellow solution was preserved in an amber-colored container and stored in a refrigerator at a temperature of 4 °C.

2.2.2. Recycled coated graphite (R-CG) preparation. Zinc/carbon waste batteries (such as triple-A batteries) were utilized to fabricate the working electrode by extracting the graphite bar using a pair of pliers. Firstly, the metal wrap was pulled off the battery by rolling the metal sheet outwards, removing the top metal cap, and pulling it out. Secondly, the plastic wrapping was removed by squeezing the top plastic ring, then squeezing the battery body from all directions to loosen the graphite rod from the center. The remaining zinc paste on the graphite rods was removed using 0.5 M H_2SO4 as a cleaning solvent to thoroughly eliminate any impurities adhered to the bar surface within 30 minutes, then resoaked in ethanol for 12 minutes and rinsed with distilled water for further elimination of any impurities. Some wax can also be removed by exposure to the heat of a torch to burn the wax off. The cleaned graphite bar was then inserted into a 5 cm long and 3 mm diameter dielectric PTFE (polytetrafluoroethylene) tube, and then the tube was exposed to the heat of a torch to shrink and firmly adhere it to the graphite electrode rod. The electrode body surface was mechanically polished using rough emery paper until a surface smoothness like a mirror was achieved; the other side of the electrode bar, about 0.5 cm, was left uncovered for connection.[30] Upon cyclic voltammetric scanning (20 cycles) within a potential window of −0.5 V to 1 V in 0.1 M NaOH at a scan rate of 100 mV s^{-1}, the recycle graphite carbon electrode was electrochemically activated until stable CV peaks were achieved.[31]

2.2.3. The R-CG@α-CD ion-selective electrode assembly. Five different sensors were utilized with different components to obtain the most precise, sensitive, and accurate results. Here, 10.0 mg of precipitated CBZ ion pair with tetraphenylborate (TPB), 0.35 mL dioctyl phthalate as a plasticizer, and 190.0 mg PVC were mixed well to fabricate the sensing membrane and then dissolved in 5 mL of THF to yield (TPB/ISM) as sensor (I). A micropipette was used to drop cast 20.0 μL of nitrogen-doped carbon quantum dots derived from pea pods (PP-NCQDs)

solution as a thin layer before adding the selective membrane layer in sensor one, and left to dry at room temperature overnight to obtain sensor (II) (TPB/PP-NCQDs/ISM). For the preparation of sensors III to V, we added 5 mg of the ionophore (α, β, or γ-CD) to the selective layer in sensor II to obtain sensors III, IV, and V, respectively.

2.2.4 Standard solutions. A CBZ stock solution was prepared by dissolving 312 mg in 100 mL of Britton Robinson buffer (BR) pH 5 to obtain a solution concentration of 1×10^{-2} M. Working solutions of progressively lower concentrations (1×10^{-3} M to 1×10^{-9} M) were prepared by serial dilution of the stock solution.

2.2.5. Potentiometric measurements. A Jenway pH meter 3510, England, was used for a potential reading study using the five main working electrodes in conjunction with a double junction reference electrode (Ag/AgCl) model. The solutions were calibrated by immersion in solutions of CBZ (1×10^{-9} to 1×10^{-2} M) under magnetic stirring till a constant emf for each solution and sensor was achieved. Calibration curves were then plotted between the recorded emf and the negative logarithmic CBZ concentration (−log) of [CBZ]. Consequently, the corresponding regression equations were calculated.

2.2.6. Quantification of CBZ in moveasy tablets. Ten tablets were finely ground, and their average weight was determined. A quantity equal to 31.2 mg of CBZ powder was precisely weighed, put into a 100 mL volumetric flask, and diluted to the appropriate level with BR, pH 5.0. The resulting CBZ solution concentration was obtained to be 1×10^{-3} M. The optimized electrode **α-CD/PP-NCQDs/R-CG** sensor, in conjunction with the double-junction Ag/AgCl reference electrode, was immersed in the prepared solution. The potentials measured were recorded to calculate the corresponding concentrations from the regression equation of that electrode.

2.2.7. Potentiometric CBZ determination in wastewater samples. Wastewater samples characterized by elevated contaminant levels were obtained from the Senhewat leakage site located in Minya Al Qamh, Egypt, with samples collected in triplicate. The wastewater samples were preserved in amber glass bottles with polypropylene open-top Teflon-silicon septa screw caps. With respect to wastewater samples, cyclobenzaprine (CBZ) demonstrates a propensity for protein binding, which warrants careful consideration during analytical evaluations. Complete denaturation of proteins is accomplished through the introduction of absolute ethanol. The role of ethanol is twofold: it aids in the denaturation of proteins and facilitates the extraction of CBZ. One ml of wastewater was mixed with suitable aliquots from the stock solution, 9 mL of absolute ethanol was added, and the mixture was agitated for 3 minutes using a vibromixer. The mixture was then incubated for 45 minutes at 60 °C in a water bath. This methodology results in the denaturation and subsequent precipitation of any minute quantity of proteins from wastewater. After the cooling stage, the ethanol phase is separated through centrifugation for 20 minutes at 3500 rpm for further analysis. This is followed by another extraction of the residue. The ethanol extracts are concentrated by evaporation. The residue dissolves in BR pH 5, and the calibration portion shows the concentration.

2.2.8. Molecular docking (MD). Molecular conformations and orientations between CBZ and its cyclodextrin (CD) hosts were determined by the Molecular Operating Environment (MOE). In this study, the structures of CBZ and cyclodextrin ionophores (α, β, and γ) were built into 2D and 3D by the MOE for binding energy calculation and fitting the properties of each ionophore to CBZ as a target ligand. The structure of each modifying ionophore and CBZ was obtained from the protein data bank (PDB) and the PubChem database. The docking process was protonated at pH 5 in the software, and partial charges were energy-minimized. The higher the docking score, the better the position and ionophore-to-ligand interaction; consequently, the more selected the ionophore in the modified electrode preparation, the more compatible the results obtained in the practical work.

3. Results and discussion

The creation of rapid and affordable analytical techniques that are free from dangerous chemicals and complex equipment is consistent with the purpose of green analytical chemistry. At the moment, all researchers worldwide are interested in these approaches. The addition of new nanomaterials like NCQDs to solid contact sensors recycled from graphite takes advantage of their remarkable benefits and enhances the electrochemical performance of the newly created sensors because carbon-based nanomaterials improve sensor performance by increasing the transduction and conductance of the chemical to an electrical signal, which lowers the detection limits. The incorporation of NCQDs into a bare graphite electrode resolved the low selectivity and sensitivity problems faced when using a bare graphite sensor alone for a target analyte.

3.1. Characterization of the pea pod-derived NCQDs (PP-NCQDs)

EDX analysis was used to verify the presence of elements such as oxygen (O), carbon (C), and nitrogen (N) in NCQDs. Since pea pods contain a lot of potassium, the EDX analysis also found trace amounts of potassium (K), which might have been the result of leftover material from the process of preparing the pods for NCQDs. However, the quantity was negligible and would not have a substantial effect on the quantum dots' surface characteristics. As seen in (Fig. 1), the presence of N components that came from NCQDs demonstrated that nitrogen was successfully incorporated onto the surface of carbon quantum dots (Fig. 1).

The morphology of the nanoscale carbon quantum dots (NCQDs) was characterized by transmission electron microscopy (TEM), as presented in Fig. S1a. The NCQDs exhibited a spherical morphology with an average particle diameter of approximately 9.6 nm. The uniform monodisperse nature of the NCQDs signifies excellent solubility in aqueous media and optimal dispersion in water. The selected area electron diffraction (SAED) pattern illustrated in Fig. S1b indicates that the concentric rings, which are characteristic of the diffraction pattern, dissipate when the carbon quantum dot (CQD) particle

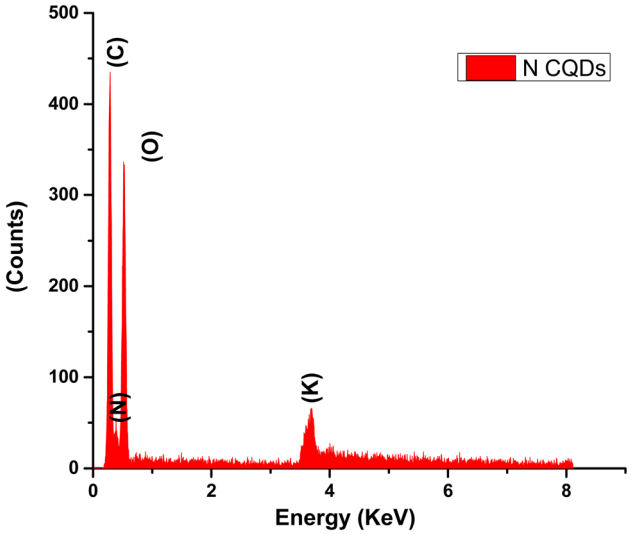

Fig. 1 EDX elemental composition analysis of PP-NCQDs.

dimensions are diminutive or entirely amorphous, resulting in a halo surrounding the luminous central point. This observation elucidates that electrons are scattered randomly due to the amorphous characteristics of the carbon dots (CODs). These findings are in substantial agreement with those obtained from X-ray diffraction (XRD) and Raman spectroscopy analyses (Fig. S1c).

To determine the crystalline architecture and phase homogeneity, the nitrogen-doped carbon dot sample was subjected to characterization employing the X-ray diffraction (XRD) methodology. Conversely, amorphous carbon quantum dots (CQDs) lack a periodic crystalline lattice,[32] are incapable of diffracting electrons,[33] and may display an X-ray diffraction profile characterized by an amorphous halo presenting a peak within the 2θ range of 21.00–21.76°, where the (002) reflection plane of graphite is associated with the broad and strong characteristic peak in this range.[34–36] As illustrated in (Fig. S1c), the obtained pattern shows a large peak at around 2θ in the range of 34.58–40.21° corresponding to the (001) reflection plane. This result illustrates how the creation of extra oxygen-containing groups results in poor crystallinity in carbon dots. The selected area electron diffraction pattern (SAED) for the amorphous nature confirmed the amorphous structure of N-CQDs. (Fig. S1d) illustrates the Fourier Transform Infrared (FT-IR) spectrum of Nitrogen-doped Carbon Quantum Dots (N-CQDs), exhibiting several distinct bands within the range of 1233 cm^{-1} to 1723 cm^{-1}, which are indicative of the characteristic stretching vibrations associated with carbon–nitrogen (C–N) bonds.[37] The bending vibrations of nitrogen–hydrogen (N–H) are also detected within the interval of 678 cm^{-1} to 840 cm^{-1}, with specific peaks at 1564 cm^{-1}, 1357 cm^{-1}, and 1233 cm^{-1} being attributed to the typical stretching modes of heterocyclic C–N–C, N–(C)3, and C–N–C bonds.[38] The pronounced absorption bands observed at 1723 cm^{-1} and 1616 cm^{-1} are ascribed to the presence of carbonyl (–C═O) and carboxylic acid (–COOH) functional groups located at the edges of N-CQDs, alongside the stretching frequency corresponding to the imine (–C═N–) formed through the condensation reaction between carboxylic acids and primary amines within the NCQD.[39] The broad peaks that manifest within the range of 3139–3539 cm^{-1} are attributed to the stretching vibrations of hydroxyl (–OH) and amine (–NH) groups, thereby suggesting the existence of multiple hydroxyl and amino functional groups within the structure of the N-CQDs. These findings demonstrated that N species were effectively doped into the structure of the CQDs and that the N-containing groups were created by a chemical interaction between L-serine and the microcrystalline cellulose of pea pods.

3.2. Recycled graphite electrode composition and optimization

The most appropriate sensor was identified by various experimental series, including ion exchangers, plasticizers, ionophores, and modifiers, to confirm maximal selectivity and

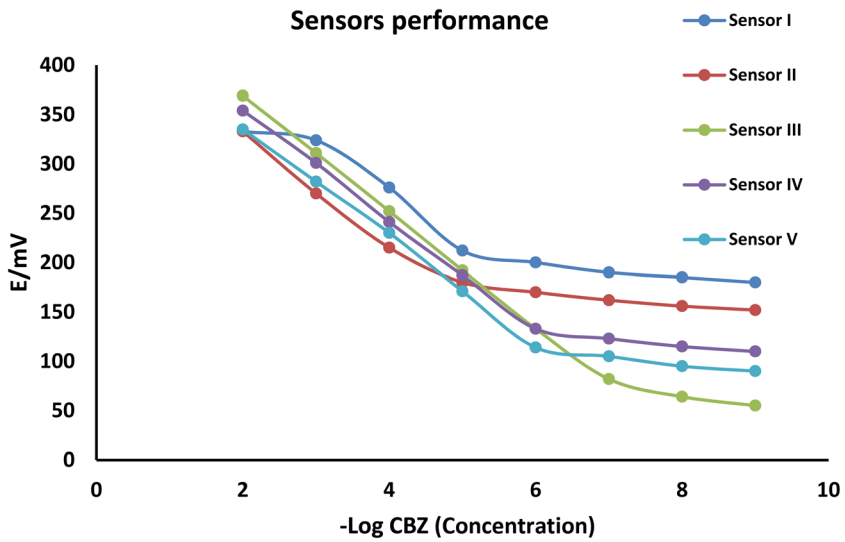

Fig. 2 Profile of the potential of the proposed sensors for CBZ determination.

sensitivity (Table S1). The electrochemical optimization for CBZ determination should incorporate an ion exchanger in its polymeric membrane, which enhances the selectivity of the membrane sensor towards CBZ; TPB showed the highest response and linearity range among the other cationic exchangers. Several plasticizers were evaluated according to their effect on electrode performance; after several trials, dioctyl phthalate (DOP) was found to be more effective than other plasticizers such as dibutyl phthalate (DBP) and tributyl phosphate (TBP). Upon inclusion of either TBP or DBP in the polymeric membrane, a non-reproducible response with a sub-Nernstian below 52.00 mV/concentration decade was found, and then both TBP and DBP were excluded for further optimization. Additionally, various experimental trials were performed to choose the most suitable ionophore, and confirmed by MD. Different cyclodextrin ionophores were used for experimental trials, such as (α, β and γ) CD and it was determined that (α -CD), functioning as an ionophore characterized by its lipophilic properties, provides numerous accessible cavities, enhances the stability of the sensor's response, and extends its operational lifespan due to its pronounced lipophilicity, which facilitates robust retention within the membrane. Furthermore, the integration of NCQDs was implemented to enhance the sensitivity of the analytical technique employed. The application of nitrogen-doped CQDs provides several benefits, such as an augmented surface area that enhances the thermal stability and a plethora of electrical attributes. By utilizing a recycled graphite-coated electrode through a drop-casting approach, the previously selected components were utilized in the fabrication of the five sensors, as delineated previously. Upon recording the variations in potential readings between all sensors as shown in Fig. 2, all proposed sensors were checked for their performance in CBZ determination, and it was found that sensor III (**α-CD@PP-NCQDs/R-CG**) showed the best and most reliable performance compared to the other proposed sensors, which increased the linearity range from 1.0×10^{-7} to 1.0×10^{-2} M CBZ, with a slope of −57.97 and a lower detection limit of 5.62×10^{-8} M as presented in (Table 1).

3.3. (α-CD/PP-NCQDs/R-CG) electrode selectivity study

The selectivity coefficient was used to investigate the selectivity of the optimum chosen sensor III (**α-CD/PP-NCQDs/R-CG**) by comparison of the same CBZ concentration used with a foreign substance (1.0×10^{-4} M), employing the separate solutions method (SSM)[40,41] for monovalent compounds, where the matched potential method (MPM)[42] was used for other components and interferents. Upon recording the potential response of the optimum sensor III in the presence of other interferents separately, the response of the (**α-CD/PP-NCQDs/R-CG**) sensor III was investigated in the presence of the main CBZ co-augmented drugs, such as paracetamol and diclofenac, in addition to tablet excipients, including inorganic and organic substances. The calculated selectivity coefficient results exhibited that the optimum sensor III is most highly selective to CBZ and did not have any significant interference from the interfering species (Table 2).

Table 1 Analytical validation parameters of the proposed electrochemical sensors

Parameter	Electrode I	Electrode II	Electrode III	Electrode IV	Electrode V
Linear response range (M)	1.0×10^{-3} to 1.0×10^{-5}	1.0×10^{-2} to 1.0×10^{-5}	1.0×10^{-2} to 1.0×10^{-7}	1.0×10^{-2} to 5.0×10^{-6}	1.0×10^{-2} to 5.0×10^{-6}
LOD (M)	6.7×10^{-6}	4.33×10^{-7}	5.62×10^{-8}	5.6×10^{-7}	5.6×10^{-7}
Slope (mV per decade)	−56.00	−51.4	−57.97	−55.76	−55.3
Intercept, mV	494.66	429.40	484.03	465.6	447.6
Correlation coefficient (r)	0.996	0.992	0.9997	0.9998	0.9996
Response time (s)	20	15	10	15	15
Stability (weeks)	4	4	6	6	6
Accuracy ± SD[a]	100.20 ± 1.895	99.40 ± 1.967	99.70 ± 0.987	99.86 ± 1.872	100.37 ± 1.376
Repeatability[b]	1.88	1.22	0.453	1.061	1.1171
Robustness[c]	1.67	1.74	0.876	1.564	1.614
Intermediate precision[d]	1.91	1.65	0.567	1.452	1.562
Reproducibility (%RSD)[e]	1.45	1.22	0.51	0.76	0.98

[a] SD mean recovery at three levels for five different concentrations. [b] %RSD for three different concentration levels in three replicates within the same day. [c] %RSD upon a small variation in method parameters such as soaking time and pH. [d] %RSD for three replicate determinations on three successive days. [e] %RSD for using six electrodes of the same composition.

Table 2 Selectivity coefficients of different interfering compounds for the CBZ sensor

	Sensor III	
Interferent	MPM	SSM
Paracetamol	1.2×10^{-3}	—
Diclofenac sodium	3.2×10^{-3}	—
Starch	8.34×10^{-3}	—
Glucose	7.96×10^{-4}	—
Sucrose	2.38×10^{-4}	—
Urea	3.17×10^{-4}	
Glycine	4.17×10^{-4}	—
$CaCl_2$	2.37×10^{-3}	—
Mg stearate	1.57×10^{-4}	—
NH_4Cl	—	1.53×10^{-4}
NaCl	—	4.93×10^{-4}
KCl	—	1.68×10^{-4}

3.4. The effect of pH

One of the most significant influences on the potentiometric response of the suggested sensor is pH. The possible response of the suggested sensor III was studied over a pH range of 2–8 in BR buffer at two intermediate concentrations (10^{-4} and 10^{-5} M of CBZ). The sensor stability readings revealed that the electrode demonstrated a stable response over the pH range of 4–6.5 (Fig. 3); above pH 6.5, the potentials presented by the sensors dropped as a result of the formation of a non-protonated compound. The release of free base inside the solution may be the cause of any potential reduction above these predetermined thresholds. The potentials that the sensors showed were imbalanced and loud below pH 4. It is evident that in pH 4–6.5 solutions, the sensor responses are comparatively consistent, and pH 5 was chosen as the intermediate and the most stable pH for potential stability.

3.5. Response time, reproducibility, robustness, and membrane electrode stability

The response time is the time needed to achieve a stable potential state (within ±1 mV) following a change in the CBZ concentration. Compared to previous sensors, which had response times of 15–30 seconds, sensor III demonstrated a quick response time of about 10 ± 1 second (Fig. S2). In order to assess the constructed electrode's repeatability, six (**α-CD/PP-NCQDs/R-CG**) sensors were fabricated under identical conditions.

Table 1 illustrates a remarkable level of reproducibility, as the sensors exhibited analogous responses, yielding a percentage relative standard deviation (%RSD) of 0.51. Robust analytical methodologies are characterized by their capacity to withstand minor alterations in procedural parameters. The potential response was systematically observed subsequent to a slight alteration to the experimental parameters to assess the effectiveness of the employed methodology. The variables scrutinized encompassed pH variation (5.0 ± 0.1) and the duration of immersion in the stock solution (24 hours ± 2 minutes). The resilience of the proposed methodology is corroborated by the lack of any impact from these minor variations on the potential response of CBZ, with %RSD remaining below 2%. The optimum sensor III that was fabricated exhibited acceptable and stable performance over 6 weeks in comparison to other electrodes (Table 1).

3.6. Water layer test

The Pretsch group created the water layer test.[43,44] A drawback of solid-contact ion-selective electrodes (SC-ISE) that restricts the potentiometric responses is the presence of an aqueous layer of water between the ion-to-electron transducer layer and beneath the polymeric membrane. Potentiometric readings were acquired for 1.0×10^{-4} M CBZ for 60 minutes, then it was

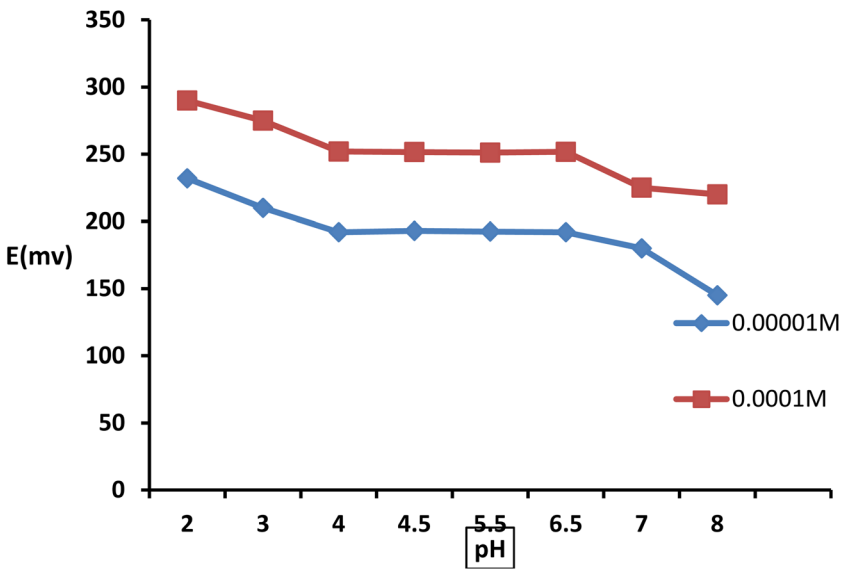

Fig. 3 The effect of pH on the **α-CD/PP-NCQDs/R-CG** (sensor III) response.

replaced with a more concentrated reference interfering solution (1.0×10^{-1} M tetrapentyl bromide), and the potential was recorded for another 60 minutes, then returned to the 1.0×10^{-4} M CBZ solution for the last 60 minutes. Upon examination of five electrodes, it was concluded that sensor 1, which did not contain NCQDs, displayed the lowest potential drift value, as shown in Fig. S3. The other electrodes modified with NCQDs enhanced the development of an aqueous layer to increase the potential drift, which was related to the hydrophilic properties of the NCQD nanomaterials in these sensors, but this high drift in the modified sensors was compensated by the higher sensitivity, conductivity, wider linear range, and low detection limit for these sensors, making them superior to sensor 1.

3.7. Molecular docking (MD)

The MD study is intended to save time and money when choosing the best ionophore CD to pick the most appropriate electrode for sensitive CBZ evaluation by determining the optimal electrode modification. Scoring functions are employed to evaluate the binding energies of the ligand within its designated binding site. Numerous scoring functions exist, yet the most prevalent is the classical force field, which evaluates the binding energies predicated on the aggregate of the non-bonded interactions, such as van der Waals and electrostatic interactions. The docking scores obtained from molecular surface interactions for (α, β, and γ) CD were determined to be −10.32, −9.55, and −9.68 kcal mol^{-1} (Fig. 5). Additionally, the molecular diameters of the host (CD) and guest (CBZ) showed that the average diameter of the inner dimension structure sizes differed, measuring 0.52 nm for the average size CBZ, 0.57 nm for α-CD, 0.78 nm for β-CD, and 0.95 nm for γ-CD. Accordingly, the best fitting one in diameter was the modified electrode with α-CD ionophore, showing the higher stability of the formed inclusion complex as a result of the perfect inclusion of the α-CD ionophore with the CBZ molecule, which is consistent with the earlier docking scores results (Fig. 4). The highest docking score (−10.32) between CBZ and the α-CD ionophore was firstly due to the nature of the strong binding between CBZ and α-CD ionophore *via* intermolecular hydrogen bonds and electrostatic interactions between the protonated nitrogen atom in the propan-1-amine branch of CBZ and the hydroxyl-methyl moiety of the α-CD ionophore as shown in (Fig. S4). Secondly, it was related to the excellent fit of the CBZ drug molecule size to the cavity size of the α-CD ionophore.

3.8. Green assessment

Each principle of Green Analytical Chemistry (GAC) is assessed according to established criteria and is allocated a numerical score that signifies its level of adherence or influence. Together, these scores create the full Analytical Green Sustainability Assessment (AGSA) scores, which are placed on a scale intended to measure the analytical methodology's overall environmental sustainability and adherence to green chemistry principles. The computation takes into account various factors, including the extent of sample processing, the toxicity of reagents, the generation of waste, energy utilization, the degree of automation, and the safety of the operator. By methodically rating an analytical method's compliance with the 12 principles of GAC discussed in more detail in Table S2, the AGSA metric offers a thorough and organized assessment of its greenness. Based on the first principle of GAC, the determination of CBZ did not require extensive sample treatment, such as solid-phase extraction, liquid–liquid extraction, and protein precipitation techniques with a small sample size. The analytical method involved instruments with low energy consumption; all samples were measured in water as a green solvent, CQDs were prepared in water as a natural solvent and environmentally sustainable recycling of spent graphite was performed. The most used reagents are less toxic, with low-risk procedures with personal protective equipment needed, as shown in Fig. 5. The AGSA tool can be used to rapidly and

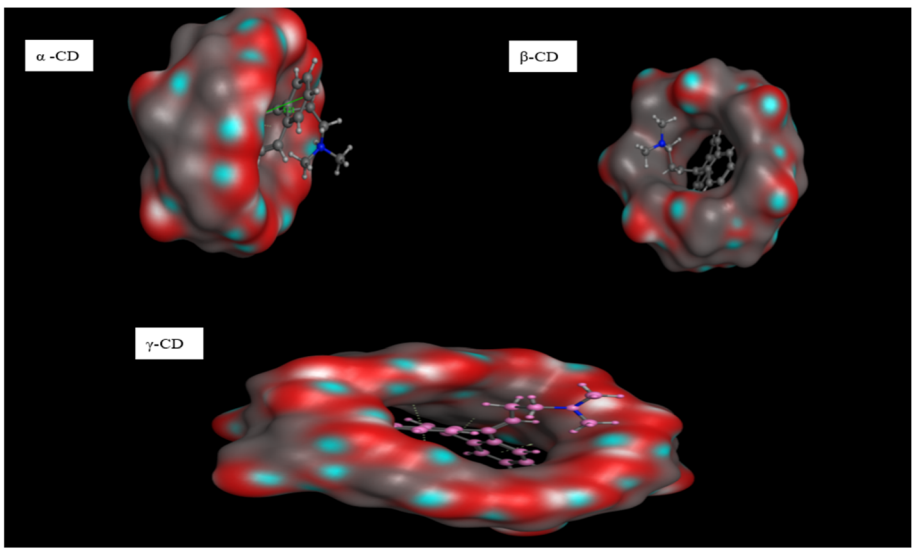

Fig. 4 Molecular surface interactions of CBZ drug binding with (α, β and γ) CD pockets.

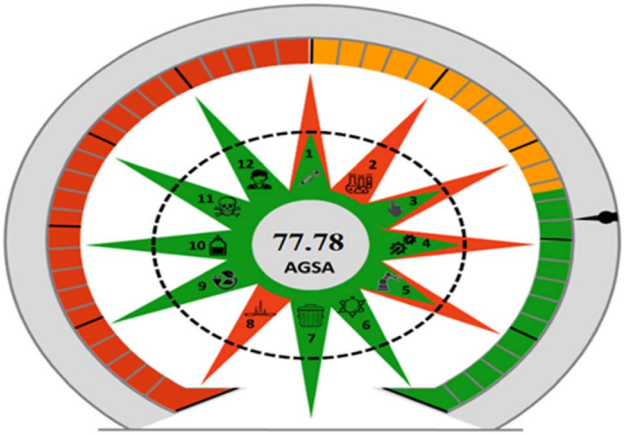

Fig. 5 Analytical green star area method metrics.

efficiently evaluate the ecological soundness of analytical methods with the use of specialized software. The final AGSA score of 77.78, as displayed in Table S2, demonstrates the outstanding applicability of the suggested technique in green chemistry. We intend to validate the AGSA tool by applying it across a series of published analytical methods to demonstrate its consistency, discriminatory power, and correlation with other green metrics in the literature. Additionally, plans include inviting the broader analytical chemistry community to contribute to refining and validating AGSA, thus fostering cross-disciplinary comparison and acceptance.

3.9. Applications

3.9.1. Determination of CBZ in Moveasy® tablets and wastewater. The employed sensor was used to quantitatively analyze CBZ in Moveasy® tablets. The results obtained for our suggested electrode showed that it is highly reliable and sensitive and that it is not affected by any additives or excipients, as shown by the recovery percentages in Table 3. Spiked wastewater samples were examined to evaluate the potential matrix effect on the sensor's performance. According to the results in Table 3, the spiked wastewater sample recovery values varied from 100.77% to 101.96%, with the %RSD values for sensor III being less than 2.

Table 3 CBZ determination in tablets and spiked wastewater

	Sensor III
Application	%recovery (mean ± %RSD)
Moveasy® tablets (10 mg per tablet)	
1.0×10^{-4} M	100.41 ± 0.22^{a}
1.0×10^{-5} M	98.32 ± 0.75^{a}
1.0×10^{-6} M	99.76 ± 0.34^{a}
Wastewater	
1.0×10^{-4} M	101.96 ± 0.99^{b}
1.0×10^{-5} M	101.43 ± 0.98^{b}
1.0×10^{-6} M	100.77 ± 1.22^{b}

[a] Average of five determinations. [b] Average of five determinations.

Table 4 Statistical data for comparison of the proposed sensor with the previously reported method

	CBZ	Reported method[26]
%mean	100.47	98.23
n	5	5
SD	0.71	0.76
Variance	0.504	0.578
Student's *t*-test (2.31)[a]	2.12	—
F-Test (6.39)[a]	1.14	—

[a] The corresponding tabulated values.

3.10. Validation and statistical analysis

Table 1 displays the characteristics of the suggested sensors, which were assessed in accordance with IUPAC recommendations.[45] The suggested sensors exhibited distinct calibration curves, as shown in Table 1 and Fig. 3, where sensor III is characterized by prolonged stability periods for six weeks and a wide range of dynamic linearity, a fast time response (10 s) in comparison to other proposed electrodes in Fig. S1, and the lowest detection limit (5.62×10^{-8} M) determined in accordance with the standards set through the identification of the intersection point resulting from two linear segment extrapolations of the calibration curve (Fig. S5).[46–51] The validation parameters were evaluated in alignment with the benchmarks outlined by the International Council for Harmonisation (ICH), which are specified in Table 1. Three distinct concentrations were accurately selected and subjected to multiple evaluations of CBZ, thereby enabling the assessment of accuracy, which is depicted in Table 1 as the percentage recovery. The experimental protocol was replicated three times for three concentration levels at three separate intervals within the same day or subjected to analysis over a continuous three-day timeframe to ensure the evaluation of the precision term through repeatability and intermediate precision, respectively. Method precision, as illustrated in Table 1, was quantified by the percentage relative standard deviation % RSD. The employed potentiometric technique for sensor III was compared with a previously documented methodology by certain statistical tools.[26] The calculated *t*- and *F*-values have been determined and recorded in Table 4, indicating the absence of statistically significant discrepancies. Furthermore, the suggested methodology displayed higher sensitivity and versatility when compared with the electrochemical techniques previously documented, as presented in Table 5.

4. General conclusion

In conclusion, five solid-contact sensors were fabricated utilizing recycled battery rods, accomplished through a straightforward and cost-effective method, in conjunction with the synthesized form derived from green sources for the waste of pea pods. All of the suggested sensors performed exceptionally well in terms of analytical figures of merit and maintained long-term stability over several weeks. They were also successfully used for the direct measurement of CBZ in pharmaceutical dosage forms and for the rapid and accurate

Table 5 Comparison of the developed method with the reported methods for CBZ determination

Materials/method	Concentration range	LOD	Matrix	Reference
GCE with carbon black (voltammetry)	2.0–20.6 μmol L^{-1}	0.63 μmol L^{-1}	Pharmaceutical, biological, and environmental samples	22
Nanozyme-doped ZnO/r-GO (voltammetry)	10×10^{-6} M to 0.6×10^{-7} M	1.6×10^{-8} M	Serum and urine samples	23
S-GCN/TiO_2 (voltammetry)	0.06–10×10^{-7} mol L^{-1}	6.4×10^{-9} mol L^{-1}	Water and pharmaceutical	24
Co_3O_4/fluoro-copolymer (voltammetry)	2.49–19.61 μg L^{-1}	2.08 μg L^{-1}	Pharmaceutical	25
(α-Mn_2O_3:Co@CNTs)	1×10^{-6} to 1×10^{-2} M	2.84×10^{-7} M	Pharmaceutical	26
Screen printed (potentiometry) (Microsized graphite sensors) (potentiometry)	1×10^{-5} to 1×10^{-2} M	6.50×10^{-6}	Spiked plasma	27
Screen printed (potentiometry)	5.0×10^{-6} to 1.0×10^{-2} M	4.95×10^{-6} M	Pharmaceutical	28
N CQDs recycled coated graphite	1×10^{-2} M to 1.0×10^{-7} M	5.62×10^{-8} M	Wastewater pharmaceutical	This study

quantification in wastewater. The modified sensor III demonstrated broader linear ranges and higher sensitivity to CBZ when compared to the unmodified electrodes.

The integration of α-CD as the ionophore in the electrode modification was supported by the molecular docking results, showing its superior binding affinity and optimal fit to CBZ. These interactions contribute significantly to the improved electrode performance, including enhanced selectivity and a broader linear detection range. The constructed sensors made it feasible to selectively detect CBZ in wastewater, medicinal formulations, and potential interferences. The developed sensors are superior to many previously published methods due to their simplicity, low cost, and miniaturization, which enable the online monitoring and analysis of environmental samples. Even though some previously reported HPLC and voltammetric methods have lower detection limits, we believe that the suggested time- and cost-effective N-doped CQD-based sensors, which are made so simple, will mark a significant advancement in the potentiometric quantification of drugs in complex matrices and pharmaceutical formulations, as well as in the regular monitoring of water quality and efficacy. The AGSA metric offers a strong foundation for evaluating the suggested electrochemical method's greenness, including both visual and quantitative information about its environmental performance.

Conflicts of interest

The authors declare that they have no known competing financial interests or personal relationships.

Data availability

The authors confirm that the data supporting the findings of this study are available within the article and its SI file. Supplementary information is available. See DOI: **https://doi.org/10.1039/d5ra04880j**.

Acknowledgements

The authors extend their appreciation to Northern Border University, Saudi Arabia, for supporting this work through project number NBU-CRP-2025-128.

References

1 P. Walakira and J. Okot-Okumu, *JASEM*, 2011, 15.
2 Y. Luo, W. Guo, H. H. Ngo, L. D. Nghiem, F. I. Hai, J. Zhang, S. Liang and X. C. Wang, *Sci. Total Environ.*, 2014, **473–474**, 619–641.
3 H. Shinn, *Natl. Oceanic Atmos. Adm.*, 2019, 1–189.
4 H. Abdel-Shafy and M. Mansour, *Egypt. J. Chem.*, 2013, **566**, 449–471.
5 X. Wang, Y. Feng, P. Dong and J. Huang, *Front. Chem.*, 2019, **7**, 671.
6 V. Georgakilas, J. A. Perman, J. Tucek and R. Zboril, *Chem. Rev.*, 2015, **115**, 4744–4822.
7 C. Zhou, S. Wu, S. Qi, W. Song and C. Sun, *J. Anal. Methods Chem.*, 2021, **2021**, 9732364.
8 K. G. Nguyen, I. A. Baragau, R. Gromicova, A. Nicolaev, S. A. J. Thomson, A. Rennie, N. P. Power, M. T. Sajjad and S. Kellici, *Sci. Rep.*, 2022, **12**, 13806.
9 H. Luo, W. Mattes, D. L. Mendrick and H. Hong, *Curr. Top. Med. Chem.*, 2016, **16**, 3636–3645.
10 R. Abdel-Hameed, A. M. Ashmawy, N. M. Abourashed, E. Ali, M. AlElaimi, B. Huwaimel, O. A. O. Alshammari, M. Abdallah, A. M. Abdelzaher and A. M. Abdel-Raoof, *Microchem. J.*, 2025, **211**, 113097.
11 A. M. Abdel-Raoof, M. M. Fouad, N. S. Rashed, N. Y. Z. Hosni, A. Elsonbaty and A. Abdel-Fattah, *RSC Adv.*, 2023, **13**, 1085–1093.
12 A. Elsonbaty, A. W. Madkour, A. M. Abdel-Raoof, A. H. Abdel-Monem and A. M. M. El-Attar, *Spectrochim. Acta, Part A*, 2022, **271**, 120897.
13 G. Bayer, *Aust. Prescr.*, 2015, **39**, 59.
14 T. Sandle, *U.S. Pharmacopeial Convention*, 2016, 1503–1505.
15 M. A. Kassem and N. E. Guesmi, *Anal. Chem. Lett.*, 2016, **6**, 657–668.
16 I. A. Naguib, E. A. Abdelaleem, F. F. Abdallah and N. W. Ali, *Anal. Chem. Lett.*, 2016, **6**, 24–34.
17 M. Constanzer, C. Chavez and B. Matuszewski, *J. Chromatogr. B:Biomed. Sci. Appl.*, 1995, **666**, 117–126.
18 N. K. Ramadan, T. A. Mohamed, R. M. Fouad and A. A. Moustafa, *J. Planar Chromatogr.–Mod. TLC*, 2017, **30**, 313–322.

19 S. Y. Al-Nami, O. A. Azher, E. Aljuhani, R. Shah, S. D. Al-Qahtani, M. E. Khalifa and N. M. El-Metwaly, *J. Electrochem. Soc.*, 2021, 168.
20 L. Chen, Z. Jiang, L. Yang, Y. Fang, S. Lu, O. U. Akakuru, S. Huang, J. Li, S. Ma and A. Wu, *Chin. J. Chem.*, 2023, **41**, 199.
21 G. M. G. Eldin, M. E. Khalifa, A. M. Munshi, A. M. Aldawsari and N. M. El-Metwaly, *Microchem. J.*, 2021, **163**, 105942.
22 J. Scremin, A. Olean-Oliveira, C. A. R. Salamanca-Neto, G. S. Ceravolo, R. F. H. Dekker, A. M. Barbosa-Dekker, C. E. Banks, M. F. S. Teixeira and E. R. Sartori, *Electrochim. Acta*, 2021, **379**, 138176.
23 Y. N. Patil, M. B. Megalamani and S. T. Nandibewoor, *Mikrochim. Acta*, 2024, **191**, 336.
24 Y. N. Patil, M. B. Megalamani, S. Nandi, S. T. Nandibewoor, V. Adimule and S. Rajendrachari, *ACS Omega*, 2024, **9**, 31657–31668.
25 M. S. Sengar, P. Kumari, N. Sengar, S. P. Satsangee and R. Jain, *Talanta*, 2025, **287**, 127636.
26 A. M. Abdel-Raoof, A. O. E. Osman, E. A. El-Desouky, A. Abdel-Fattah, R. F. Abdul-Kareem and E. Elgazzar, *RSC Adv.*, 2020, **10**, 24985–24993.
27 N. K. Ramadan, H. E. Zaazaa and H. A. Merey, *J. AOAC Int.*, 2011, **94**, 1807–1814.
28 E. Y. Frag, M. E. Mohamed, R. M. Abdel Hameed and A. M. Mahmoud, *Appl. Organomet. Chem.*, 2020, **34**, 5439.
29 F. Mansour, A. Bedair, F. Belal, G. Magdy and M. Locatelli, *Sustainable Chem. Pharm.*, 2025, **46**, 102051.
30 A. G. A. El-Nasser, M. G. Metwally, A. A. Shoukry and R. M. El Nashar, *Sci. Rep.*, 2024, **14**, 29304.
31 K. Tyszczuk-Rotko, J. Kozak and A. Węzińska, *Appl. Sci.*, 2021, **11**, 9908.
32 Z. Zhang, J. Chen, Y. Duan, W. Liu, D. Li, Z. Yan and K. Yang, *Lumin.*, 2018, **33**, 318–325.
33 C. Cheng, Y. Shi, M. Li, M. Xing and Q. Wu, *Mater. Sci. Eng., C*, 2017, **79**, 473–480.
34 G. Wu, M. Feng and H. Zhan, *RSC Adv.*, 2015, **5**, 44636–44641.
35 M. A. Chaudhry, R. Hussain and F. K. Butt, *Metal Oxide-Carbon Hybrid Materials*, 2022, pp. 547–559.
36 M. Nagaraj, S. Ramalingam, C. Murugan, S. Aldawood, J. O. Jin, I. Choi and M. Kim, *Environ. Res.*, 2022, 212.
37 J. Liu, Y. Liu, N. Liu, Y. Han, X. Zhang, H. Huang, Y. Lifshitz, S. T. Lee, J. Zhong and Z. Kang, *Science*, 2015, **347**, 970–974.
38 A. Cai, Q. Wang, Y. Chang and X. Wang, *J. Alloys Compd.*, 2017, **692**, 183–189.
39 D. Sengottuvelu, A. K. Shaik, S. Mishra, H. Ahmad, M. Abbaszadeh, N. I. Hammer and S. Kundu, *ACS Omega*, 2022, **7**, 27742–27754.
40 M. S. Eissa, A. M. Abdel-Raoof, K. Attala, M. M. El-Henawee and S. S. Abd El-Hay, *Microchem. J.*, 2020, **159**, 105363.
41 T. S. Ma and S. S. M. Hassan, *Organic analysis using ion-selective electrodes*, Academic Press, London, 1982, vol. 2, ch. 14.
42 J. Sutter, A. Radu, S. Peper, E. Bakker and E. Pretsch, *Anal. Chim. Acta*, 2004, **523**, 53–59.
43 M. Fibbioli, W. E. Morf, M. Badertscher, N. F. De Rooij and E. Pretsch, *Electroanalysis*, 2000, **12**, 1286–1292.
44 J. P. Veder, R. De Marco, G. Clarke, R. Chester, A. Nelson, K. Prince, E. Pretsch and E. Bakker, *Anal. Chem.*, 2008, **80**, 6731–6740.
45 N. G. Connelly, T. Damhus, R. M. Hartshorn and A. T. Hutton, *Nomenclature of Inorganic Chemistry, IUPAC Recommendations 2005*, RSC Publishing, 2005.
46 R. Abdel-Hameed, A. Hegazy, E. Ali, A. M. Ashmawy, B. Huwaimel, K. D. Alanazi, M. H. Almabadi, M. AlElaimi, A. S. Eissa, A. M. Abdelzaher and A. M. Abdel-Raoof, *Microchem. J.*, 2025, **216**, 114589.
47 B. Chandran, S. Ramasamy, P. Sathish Kumar, A. Elangovan, S. Chandrasekaran, S. Karuppaiah and A. Ganesan, *ACS Appl. Nano Mater.*, 2024, **7**, 6839.
48 B. Shobana, P. Sathish Kumar, K. Renugadevi and P. Prakash, *Food Chem.*, 2024, **439**, 138073.
49 K. Alagumalai, S. Palanisamy, P. S. Kumar, N. A. ElNaker, S.-C. Kim, M. Chiesa and P. Prakash, *Environ. Pollut.*, 2024, **343**, 123189.
50 C. Bhuvaneswari, R. Shanmugam, A. Elangovan, P. Sathish Kumar, C. Sharmila, K. Sudha, G. Arivazhagan and P. Subramanian, *Food Chem.*, 2024, **437**, 137874.
51 B. Shobana, L. Gayathri, P. Sathish Kumar and P. Prakash, *Microchem. J.*, 2023, **193**, 109116.